Timothy C. Mills, PhD • Douglas A. Ortendahl, PhD • Nola M. Hylton, PhD
• Lawrence E. Crooks, PhD • Joseph W. Carlson, PhD • Leon Kaufman, PhD

Partial Flip Angle MR Imaging[1]

Theoretical analysis predicts that performing magnetic resonance (MR) imaging with partial (<90°) flip angles can reduce imaging times two- to fourfold when lesions with elevated T1 values are being examined. This time savings occurs because repetition time (TR) is reduced when imaging is performed with partial flips. Partial flip MR imaging can also improve signal-to-noise ratio (S/N) in fast body imaging. For this study, analytical tools were used to predict image contrast and S/N for short TR, partial flip sequences. Experimental implementation of the short TR, partial flip sequences that analytical work had predicted would be optimal supported the analytical predictions and demonstrated their validity. Partial flip MR imaging is applicable to reducing imaging time only when the ratio of signal differences to noise exceeds threshold values in conventional MR images. Partial flip sequences can be used to advantage in MR imaging of both the head and the body, and the observed effects are predictable through theoretical analysis.

Index term: Magnetic resonance (MR), technology

Radiology 1987; 162:531-539

THE THROUGHPUT of patients in MR imaging departments is governed by three factors: imaging time, data flow through time, and patient handling time. As imaging times continue to decrease, their impact on throughput becomes less important. Nevertheless, there are benefits to reducing imaging time, especially in studies in children, in seriously ill patients, and in anxious, uncooperative, or cognitively deficient patients. In studies in which the goal is to detect changes in tissue composition, reducing imaging time poses significant challenges. In the head, for instance, experimental (1, 2) and analytical (3, 4) studies demonstrate that sequences with a long repetition time (TR) are needed for the detection of subtle compositional differences in brain parenchyma. With present two-dimensional (2D) Fourier transform imaging techniques, long TR values imply long imaging times. Fortunately, because of the introduction of multisectional imaging (5, 6), the impact on throughput of these long TR techniques is not serious.

The detection of pathologic conditions of the brain with the use of MR contrast media that shorten T1 has led to an expectation that shorter TR techniques may be sufficient. This does not appear to be the case. A recent study of MR imaging in 30 patients in which both short and long TR sequences were used, both with and without the administration of contrast media in the patients, found that contrast-enhanced short TR sequences missed half of the intraaxial lesions detected with unenhanced long TR sequences and that the combination of contrast enhancement and long TR could make some lesions undetectable (7). Other research also leads to the conclusion that the use of contrast media will increase study time rather than shorten it (8). These considerations argue for a continued search for sensitive but fast MR imaging sequences.

An MR image is characterized by three factors: its spatial resolution, its object contrast level, and its signal-to-noise ratio (S/N) (in which the term "noise" includes both normally distributed noise and texture or artifacts). Conventional 2D Fourier transform MR imaging can be sped up by reducing spatial resolution for a given field of view or by shortening TR. A shortened TR, however, reduces object contrast for pathologic conditions of the brain in a well-understood way (1-4) and reduces S/N per unit area. It is worth noting, though, that for any given resolution and contrast, S/N need reach only a level sufficient for confident detection; above that level, further increases in S/N make the image more pleasant but not more efficacious. Today, with the high S/N levels available at medium magnetic field strength, the head can be covered optimally (for 3.5 kG [0.35 T]) with a 2/30 (TR sec/echo time [TE] msec) technique in 4.3 minutes for high-resolution imaging (0.9 mm), and 2.1 minutes for regular resolution (1.7 mm). These speeds are achieved through the use of single acquisitions of each different phase-encoding projection ($n = 1$), coupled with conjugate synthesis (i.e., acquisition of one half of the data in Fourier space and generation by software of the other half prior to 2D reconstruction via Fourier transform; this process effectively reduces n to $\frac{1}{2}$), thus reducing imaging time by nearly a half without affecting spatial resolution or contrast; only S/N is sacrificed, and that in direct proportion to the square root of the imaging time (9).

With the needs of special patient populations in mind, we have continued to explore methods to further reduce imaging time. One such method is partial flip angle imaging, a technique in which angles of less than 90° are used in the rotation of

[1] From the Radiologic Imaging Laboratory, University of California, San Francisco, 400 Grandview Drive, South San Francisco, CA 94080. Received June 11, 1986; first revision requested July 25; final revision received October 14; accepted October 17. Supported in part by USPHS grant CA 32850 from the National Cancer Institute (Department of Health and Human Services), by Diasonics, Inc., and by USPHS RCDA GM00943 from the National Institute of General Medical Sciences (Department of Health and Human Services). **Address reprint requests to** D.A.O.

the sample's magnetization vector. We show that the effects of changing flip angle in MR imaging of both phantoms and humans can be predicted from a data base of conventional spin-echo images. On the basis of these predictions, the impact on S/N and contrast as flip angle and TR are varied can be studied analytically, obviating extensive experimental work and providing an avenue for the exploration of different applications.

METHODS

Analytical Methods

Conventional 2D Fourier transform imaging is performed with a flip angle of 90°. Such an angle produces maximal signal levels when TR is much longer than T1. Smaller flip angles have been used for MR imaging (10). It has become well known (11), and is exploited in spectroscopy, that maximal signals are obtained for a flip angle θ smaller than 90° when TR is less than T1. For a free induction decay, signal intensity I has a functional dependence on T1 and TR which is of the form

$$I \propto \frac{\sin\theta[1 - \exp(-TR/T1)]}{1 - \cos\theta \exp(-TR/T1)}. \quad (1)$$

Note that S/N can be maximized for any one tissue by varying θ such that

$$\theta = \arccos[\exp(-TR/T1)]. \quad (2)$$

For TR = T1 this expression has a maximum at θ = 68°.

Equation (1) also applies when a spin echo is obtained with the use of gradient reversals (rather than 180° radio frequency [RF] pulses) to refocus the magnetization. Because a spin echo rather than a free induction decay is used for data collection, the result of equation (1) is multiplied by exp (−TE/T2*). The equation thus obtained applies when T2* is much shorter than TR. The situation for RF refocusing of the spin echo is far more complex and is treated in detail in Appendix A. The work reported here centers on the use of gradient reversals.

While equation (2) describes the conditions for obtaining maximal S/N from a single tissue, in MR imaging we are concerned with the ratio of the signal difference between tissue pairs to noise (SD/N). (Note: SD/N = C × S/N, where C = the level of contrast.) As we have discussed previously (3), for a given set of imaging conditions the SD/N determines the confidence of detection of the tissue pair, and the SD/N number can be referred to as the "confidence factor." Finding optimal values for θ then becomes a more complex task, since optimal θ depends on T1, T2, and N(H) of tissues, as well as on TR and TE. If TE is fixed at near 20 msec, the point at which fat and water protons are in phase at our 3.5-kG (0.35-T) operating field, a 2D space in TR, θ must still be explored for any one pair. Since TR values between 100 msec and 2 sec are conceivably of interest, these may need to be sampled at 100-msec intervals for 20 points along the TR axis. Angles between 5° and 90° are of interest, and if sampling is done at every 5°, then 18 points need to be sampled along the θ axis, for a total of 360 points in the TR, θ plane—an imposing task if it is to be done exhaustively by experimentation.

To evaluate the potential of partial flip MR imaging under realistic conditions we modified existing analytical tools (3) to yield maps of SD/N based on T1, T2, and N(H) data obtained directly from multisectional patient studies with 2/30 and 60 and 0.5/30 acquisitions. On the basis of these maps (each of which depended on a selected tissue pair), images simulating partial flip MR imaging were calculated on a pixel-by-pixel basis so that we could evaluate the overall impact of favorable TR, θ combinations. The results of such an evaluation have been previously reported (12). A typical map of signal difference for gray/white matter is shown in Figure 1. Calculated partial flip images are presented in Results.

The results of the previously reported study can be summarized as follows: A consistent trend is found in the TR, θ map. The line of constant signal difference runs toward shorter TR values as θ decreases from 90°, but at a given TR it becomes parallel to the θ axis and then runs nearly parallel to the TR axis and toward long TR values if θ decreases further (Fig. 1). The turnover or reversal point in-

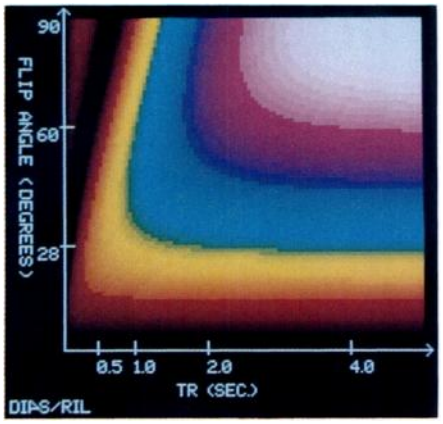

Figure 1. Signal difference map for gray and white matter, as a function of TR (0–5 sec along the horizontal axis) and θ (0°–90° along the vertical axis). The color scale shows low signal difference as red, increasing through yellow, green, blue, and violet, to white for highest signal difference.

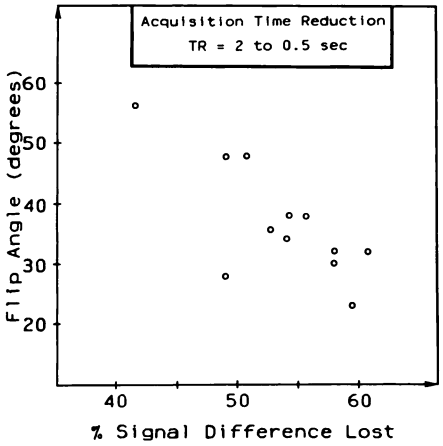

Figure 2. Loss of signal difference (assuming the same noise in partial flip and conventional MR imaging) as a function of flip angle when TR is reduced from 2 to 0.5 sec.

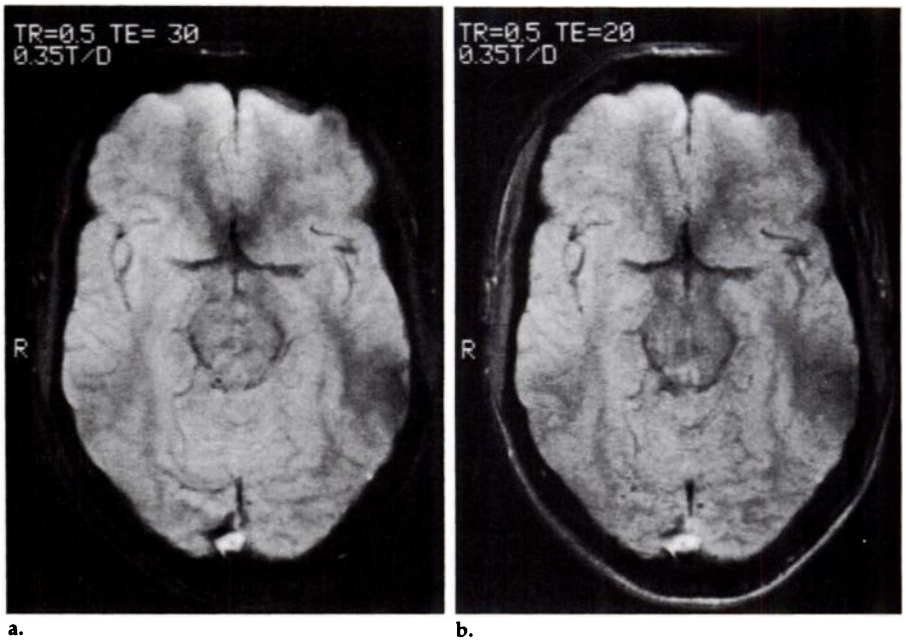

a. b.

Figure 3. Comparison in a healthy volunteer of partial flip images of the head acquired with TE = 30 msec **(a)** and 20 msec **(b)**. SD/N for gray/white matter is improved by 63% for the longer TE procedure.

dicates the optimal TR, θ point for the particular tissue pair. Fifteen patients with pathologic conditions of the head and neck were evaluated retrospectively. We found that preserving the signal difference of a TR = 2 sec procedure was not profitable since most lesion/normal-tissue plots clustered near $\theta = 70°$, for a time savings of 10%, (i.e., for TR = 1.8 sec). On the other hand, if a loss in signal difference of about 55% was allowed, then a fourfold savings in time (from TR = 2 to TR = 0.5 sec) was possible for flip angles of about 30° (Fig. 2). Figure 2 also makes it clear that if a fourfold reduction in TR is desired (from TR = 2 to TR = 0.5 sec) the signal difference of the longer TR procedure cannot be maintained at any flip angle. These results were arrived at with the assumption of a fixed number of acquisitions (n), and a fixed TE (and with them, a fixed N); the time savings is realized from shortening TR only. Because today a common acquisition method is with $n = 2$, and because we are interested in using the partial flip technique in a mode that is as rapid as possible, we compared partial flip MR imaging with $n = 1$ to the common TR = 2 sec, $n = 2$ sequences in use. The typical 55% loss in SD/N found from Figure 2 would then be expected to increase to about 77% when TE is constant.

It might be questioned whether such a loss is affordable. First, we note that we assumed in the analysis that for a given n the noise is the same in the partial flip and conventional images. This need not be the case, since the use of gradient reversals allows for longer times to sample the spin echo, with consequent reductions in noise. Therefore, for equal imaging times, partial flip images can have a higher S/N than conventional spin echo images, partially compensating for the loss of signal difference. Second, increasing the confidence factor does not increase diagnostic efficacy once a sufficiently high confidence factor is reached. For instance, for an S/N = 30 and a contrast of 20%, the SD/N, and hence the confidence factor, is 6. At such a confidence level, a false alarm will occur once in every billion pixels. If a head covers an area of 30,000 pixels, a false alarm due to random noise will occur once in every 33,000 images, or, approximately, once in every 2,000 patients. If lesions are diagnosed only when at least two contiguous pixels show a difference from background, false alarms will be reduced by eight orders of magnitude. Clearly, a doubling in confidence factor will have little impact on diagnostic confidence. Conversely, if confidence is high, halving it will not be detrimental to diagnosis. Typically, confidence factors of 4–5 are considered adequate for diagnostic imaging.

It could be argued that just reducing the number of acquisitions in the TR = 2 sec image by a factor of four would accomplish the same reduction in SD/N as a TR = 0.5 sec, $\theta = 30°$ procedure. We do not know how to do this with 2D Fourier transform imaging once $n = 1$ or $n = \frac{1}{2}$ (9). Hybrid techniques (13) can reduce imaging time further (with consequent changes in object contrast and spatial resolution functions), but the partial flip considerations apply to hybrid imaging as well. Therefore, for a unit that operates above diagnostic thresholds with $n = 1$ or $n = \frac{1}{2}$, whether in a hybrid mode or not, partial flip MR imaging can reduce imaging time. If the unit necessitates operation with $n = 2$ to be above threshold confidence factors, then a simpler strategy is

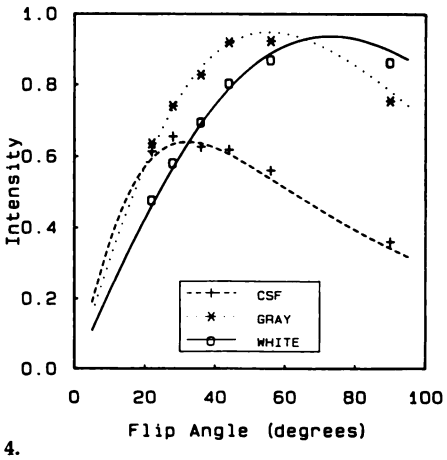

4.

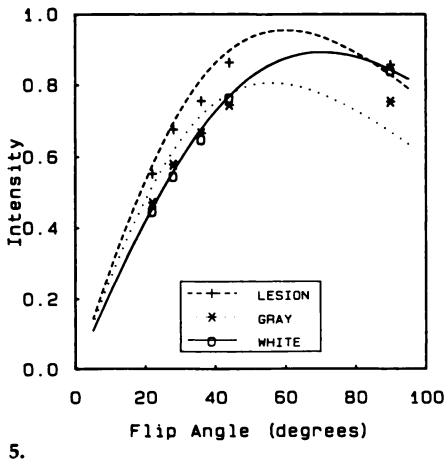

5.

Figures 4, 5. **(4)** Measured (data points) and predicted (lines) signal intensities as a function of flip angle for gray matter, white matter, and CSF in a healthy volunteer. Acquisition was performed with 0.5/20. **(5)** Measured (data points) and predicted (lines) intensities as a function of flip angle in a patient with multiple sclerosis. Acquisition was performed with a 0.5/20 sequence. Below $\theta = 60°$ the lesion becomes more intense than gray or white matter.

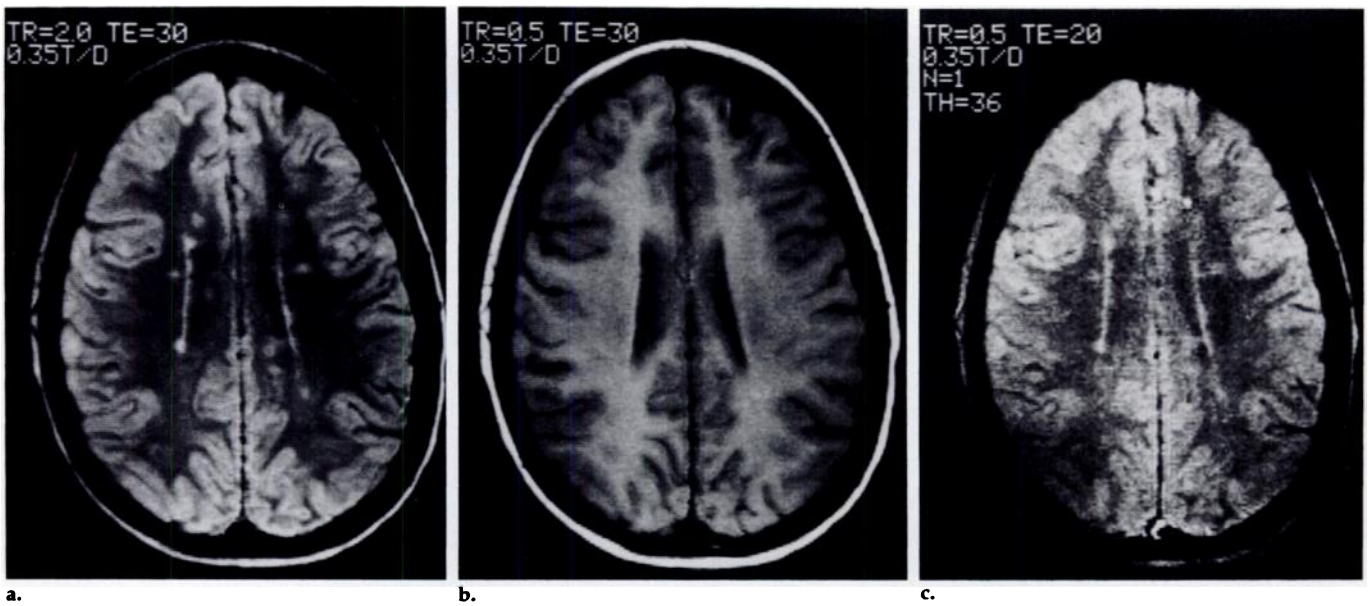

a. b. c.

Figure 6. Conventional TR = 2 sec **(a)** and TR = 0.5 sec **(b)** images in the patient with MS in Figure 5. Note normal appearance of the short TR image **(b).** With a partial flip of 36° and TR = 0.5 sec **(c),** lesions become visible. Image in **c** was acquired with the same spatial resolution parameters in $\frac{1}{8}$ the time of the image in **a**.

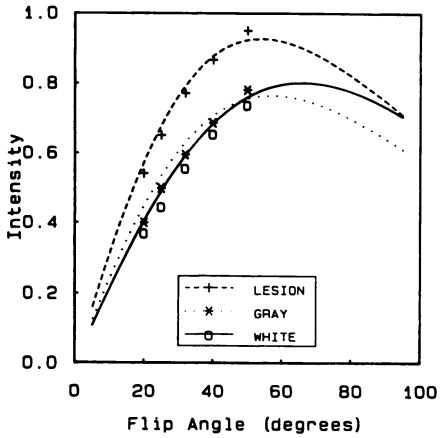

Figure 7. Measured (data points) and predicted (lines) signal intensities as a function of flip angle for a patient with an infarct. Behavior is similar to that for imaging in patient with multiple sclerosis.

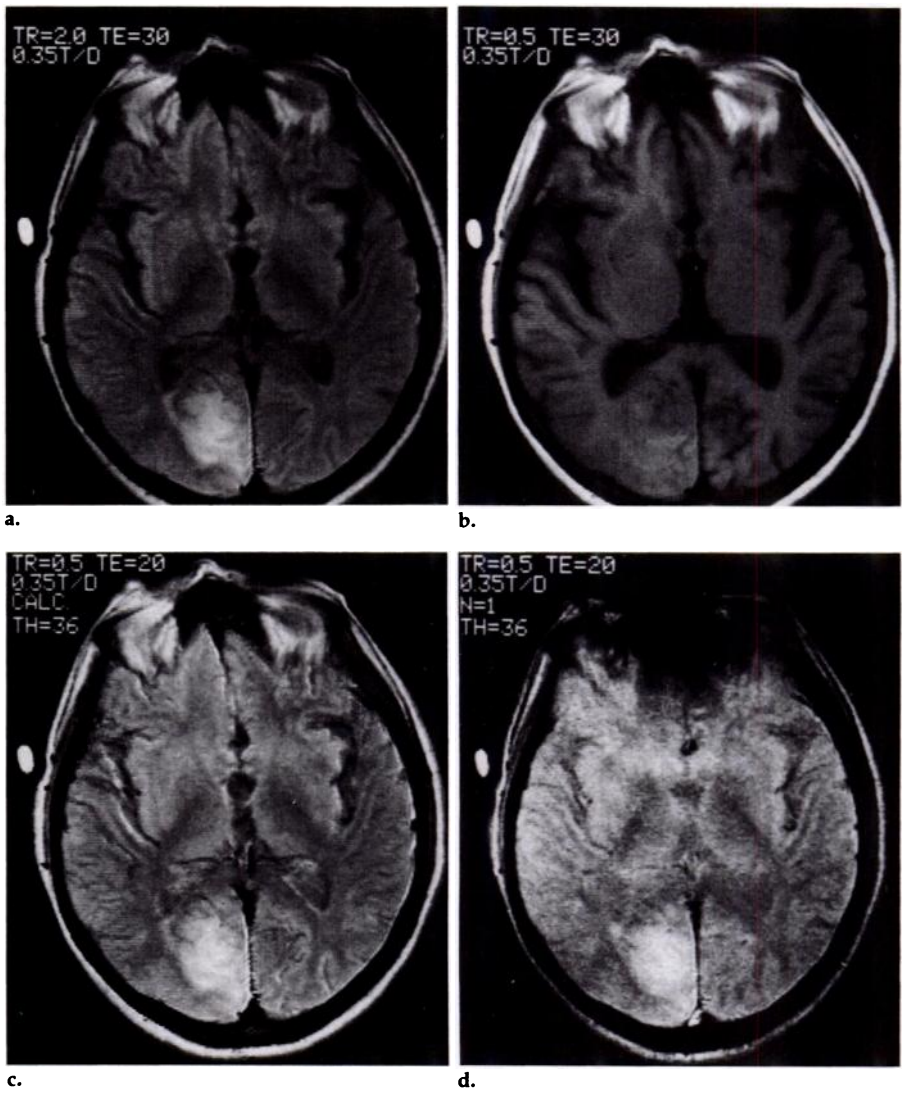

Figure 8. Comparison of acquired and predicted images for the patient with a brain infarct in Figure 7. A conventional set of 2/30 **(a)** and 0.5/30 **(b)** images are shown. From these (and a 2/60 image not shown) are calculated T1, T2, and N(H) images that lead to predicted images. Bottom row shows predicted **(c)** and acquired **(d)** images for a flip angle of 36°. S/N is higher in calculated images because they derive from longer data acquisitions. Note that in acquired partial flip image the region between the eyes shows no signal. This is the result of magnetic field distortion caused by a small dental prosthesis that does not affect conventional procedures.

to operate with the reduced values of n.

With TR = 500 msec for partial flip head imaging, we found that an optimal angle was about 30°. We also investigated analytically whether T1 calculations could be performed from two images at constant TR but different θ, as opposed to our method of TR = 0.5 and 2 sec at θ = 90° (14). We found that for equal imaging times the reproducibility of T1 measurements would be better with the conventional techniques for T1 < 1 sec, and better with partial flip MR imaging for T1 > 1 sec. At 3.5 kG (0.35 T) normal tissues are below this break-even value but the use of partial flip imaging would seem to confer an advantage for tissues with long T1 values. Nevertheless, the partial flip technique is, as could be expected, much more sensitive to RF field inhomogeneities. Our analysis indicates that for conventional TR = 2 and 0.5 sec measurements a 3° error in flip angle would result in a 2%–5% systematic error in T1 for tissues with T1 = 300–1,000 msec, but that for a TR = 0.5 sec procedure with θ = 30° and 90° the systematic error would be 11%–9%, respectively (12).

Laboratory Methods

The partial flip technique was incorporated into a prototype MT/S imager (Diasonics, Milpitas, Cal) operating at 3.5 kG (0.35 T). The conventional program for setting RF power levels was used to find the θ = 90° flip angle. At first a manually controlled attenuator was used to reduce power to achieve the desired angle; this task was later accomplished with a software-controlled parameter change.

Most of the work was performed with TE = 20 msec, so that signals from water and fat were recorded in phase when gradient reversals were used. (Note that this effect is not the same as the familiar chemical shift displacement that blurs images obtained at high fields.) Nevertheless, in the head, object contrast characteristics improved for longer values of TE, so that TE = 30 msec was advantageous (Fig. 3). Compared with TE = 20 msec images, the TE = 30 msec images had 43% higher gray/white-matter contrast and 14% higher S/N, so that SD/N was 63% higher. For a TR of 0.5 sec, the number of sections that could be obtained simultaneously was 12 with TE = 20 msec and 10 with TE = 30 msec. Phase cancellation for TE = 30 msec images appeared as dark lines at the interface of water and fat (15), most noticeably near the eyes, and did not appear in brain parenchyma. For imaging of the body we used 0.15/20 with three sections, and 0.15/12 with four sections. All acquisitions were with n = 1. In the head, spatial resolution was 0.9 mm (256 × 256 matrix) and in the body 1.7 mm (256 × 128 matrix), both with a 10-mm section thickness. Conventional 2D Fourier transform techniques were used to obtain intensity images that could then be used to calculate T1, T2, and N(H) images. Signal difference was measured as the difference in signal intensity between two target tissues. Noise was measured as the mean intensity of the signal in air, in an area of the image away from phase encoding artifacts. This measure overestimates noise slightly, the overestimate being the same in partial flip and spin-echo images.

RESULTS

Head Imaging

Figure 4 compares acquired and predicted signal intensities for gray matter, white matter, and cerebrospinal fluid (CSF) for TE = 20 msec MR imaging in a healthy volunteer. The prediction is based on T1, T2, and N(H) values obtained in a routine multisectional study. (A small [typi-

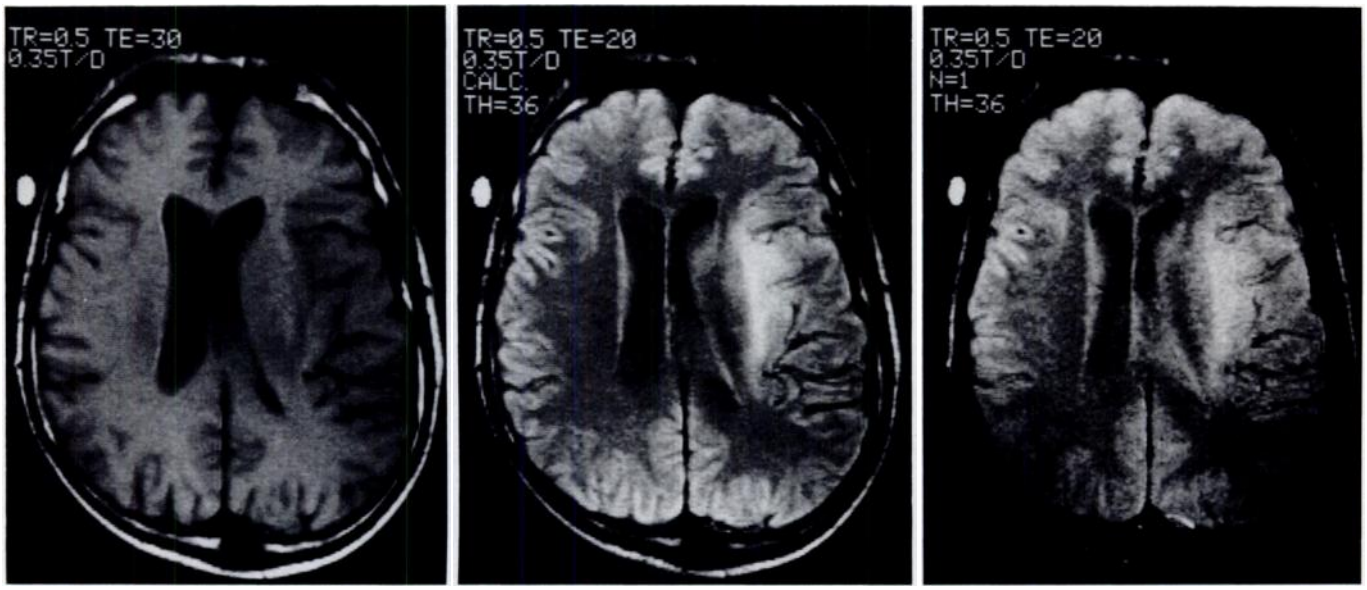

a. b. c.

Figure 9. Patient with a large tumor. Conventional TR = 0.5 sec image **(a)** shows mass effect but no abnormal signal intensities. Predicted $\theta = 36°$, TR = 0.5 sec image **(b)** shows tumor as high signal intensity. Image acquired with these parameters **(c)** produces expected appearance of the lesion.

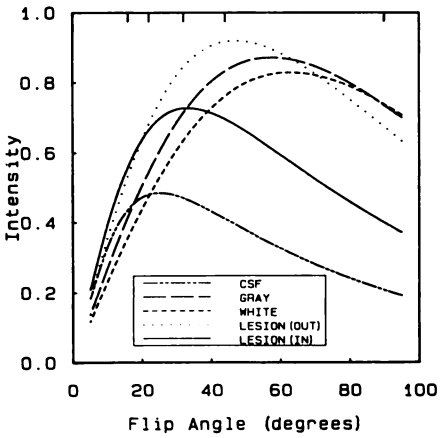

Figure 10. Fitted lines through acquired data (acquisition points indicated by tick marks on top border of the graph) show signal intensities as a function of flip angle for a patient with a brain neoplasm (inner part of the lesion) and surrounding edema (outer part). Signal differences in the region of $\theta = 30°$ are comparable to those of a long TR, relatively short echo image. Near $\theta = 20°$ the appearance of image is like that of a later echo image.

cally 10%] scale factor correction was applied to the predicted values to optimize the match to the data points. This scale factor is the same for all tissues and its need arises from uncertainties in resolution calibration when tuning the gradient reversal sequence.) Note that at a 90° flip angle the typical TR = 0.5 sec pattern is seen, a pattern in which white matter is slightly more intense than gray matter and CSF is of very low intensity. As flip angle is decreased, signal intensities peak and start to decrease. At about 65° gray and white matter are isointense, and below 50° gray

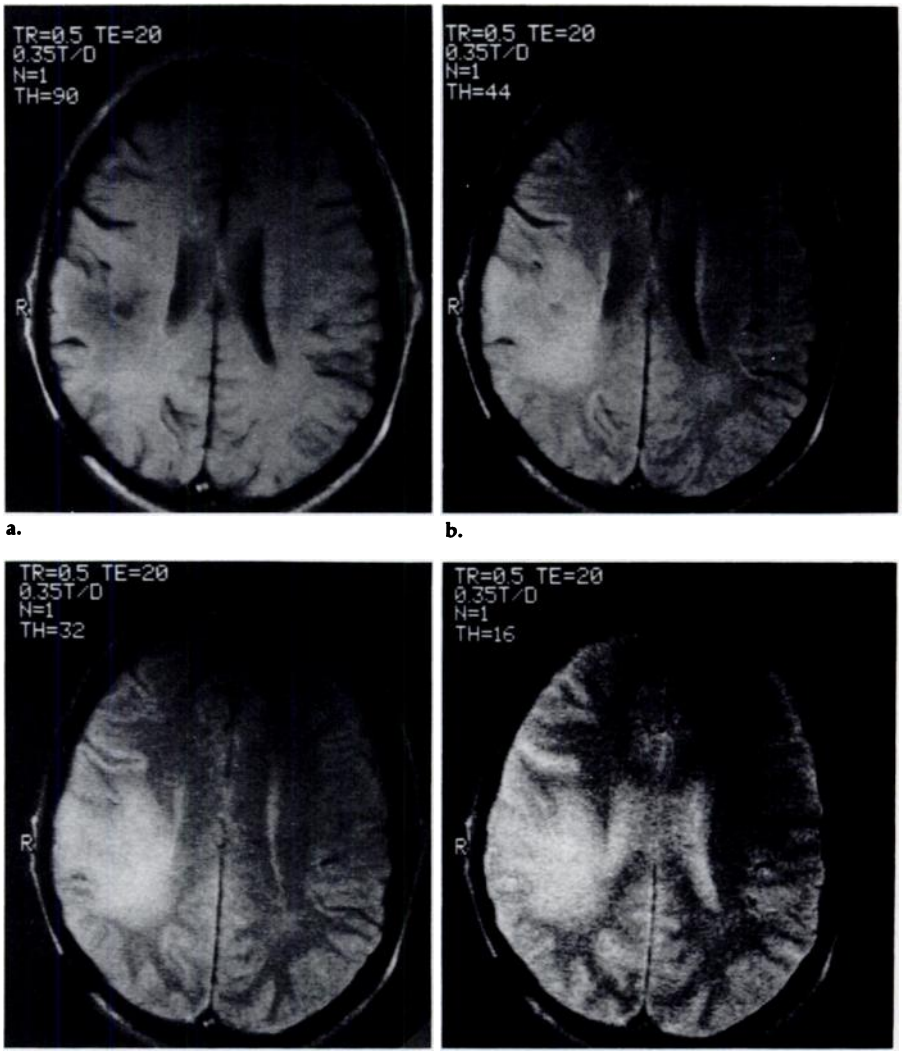

a. b. c. d.

Figure 11. Acquired images in patient described in Figure 10. Flip angles vary from 90° to 16°. A ring of high signal intensity is well seen around tumor for $\theta = 90°$ and is still apparent for $\theta = 44°$. This ring enhanced following administration of gadolinium-diethylenetriaminepentaacetic acid, a pattern observed in other patients in whom such a ring is seen.

matter is more intense than white matter. CSF becomes isointense with white matter at about 30°, and with gray matter at 20°. Qualitatively, the relationships in intensity near the 30° flip angle are similar to those of a 2/60 conventional spin-echo image. (For TE = 30 msec signal differences would be improved.)

Figure 5 shows the behavior of measured and predicted intensity as a function of flip angle for imaging of a patient with multiple sclerosis. As is typical of a TR = 0.5 sec, θ = 90°, flip angle image, the lesion is isointense with white matter. Below θ = 60°, the lesion becomes more intense than gray or white matter. Figure 6 shows conventional TR = 2 and 0.5 sec images in this patient. Notice that for the shorter TR the brain appears normal. A 0.5/20, θ = 36° image shows the lesions. The acquisition time for the 0.5/20 partial flip image is 2.1 minutes. However, a 2/20 sequence would have SD/N = 20.6 (per pixel), while the 0.5/20 image has SD/N = 5 (a 75% loss). When adjusted to the same imaging time, the partial flip image shows SD/N = 14 (32% loss).

Figure 7 compares acquired and predicted data from imaging in a patient with an infarct: The behavior is similar to that in the imaging of the patient with multiple sclerosis. Figures 8 and 9 compare acquired and predicted partial flip images for the patient in Figure 7 and another patient with a tumor. In the imaging in the patient with an infarct (Fig. 8), SD/N = 42.4 (per pixel) for the TR = 2 sec procedure and SD/N = 11.6 for the partial flip sequence (73% loss). When adjusted to the same imaging time, the partial flip procedure has SD/N = 32.7 (23% loss). For imaging in the patient with a tumor (Fig. 9), the TR = 2 sec and partial flip images have SD/N of 25.2 and 6.8, respectively (73% loss). At equal imaging times the partial flip sequence shows a 23% loss in SD/N.

A more complex case is presented in Figure 10, which shows signal behavior in imaging of a patient with a brain neoplasm (inner part of the lesion) and surrounding edema (outer part). At the 90° flip angle, for TR = 0.5 sec, the edema is slightly less intense than gray and white matter, and the tumor is much less intense, but brighter than CSF. Edema becomes more intense than gray and white matter near θ = 60°. Tumor is isointense with white matter near θ = 40°, and with gray matter near θ = 30°. Below θ = 20°, the inner and outer components of the lesions are nearly isointense, which is consistent with what is observed in an image acquired with 2/80. Figure 11 shows partial flip images obtained in this patient. For the edema/white matter, SD/N values are above 5 between flip angles of 22° and 32°.

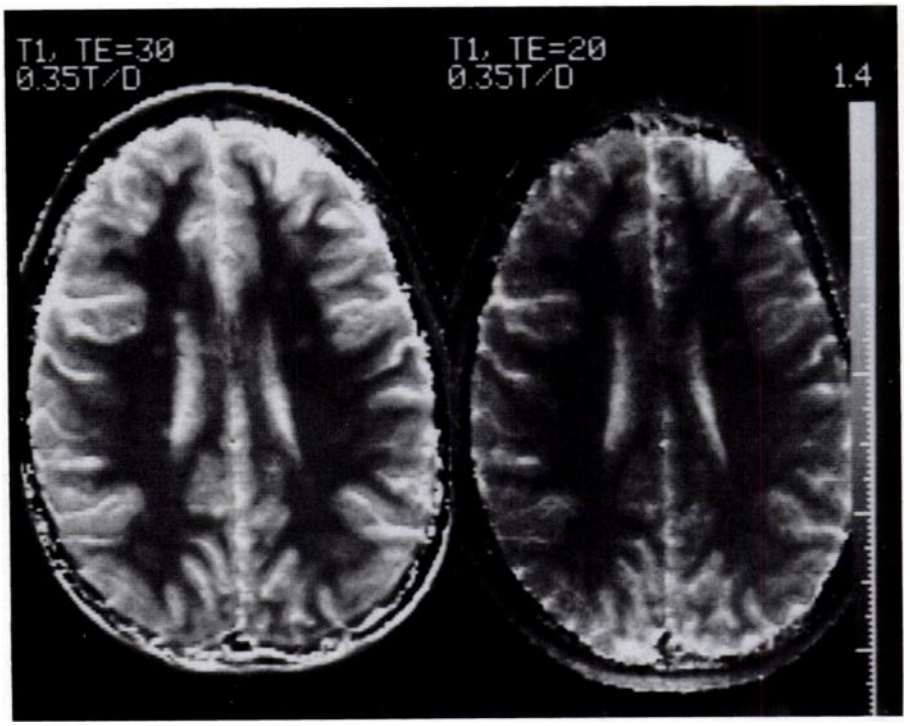

Figure 12. T1 images for patient with multiple sclerosis calculated from two TR = 0.5 sec, 2.1 min acquisitions, each with flip angles of 90° and 36°. Note uniformity of intensities (i.e., uniform T1 values).

Consistent with predictions, reducing imaging time by a factor of eight results in a 75% loss of SD/N, but SD/N remains over diagnostic thresholds. Increasing TE to 30 msec limits the loss in SD/N to under 50%. Given the high levels of confidence found in our system when used with TR = 2 sec, n = 2 imaging, such a loss is generally acceptable.

The qualitative aspects of our results in the imaging of the head can be summarized as follows. For TR = 0.5 sec, flip angles in the range of 30° provide object contrast characteristics similar to those of a long TR (1.5–2 sec) early-echo image. As the flip angle decreases to 20°, the appearance of the image changes to approximate that of a later echo image. While it would be convenient to find parameters for partial flip imaging that would exactly match certain TR/TE combinations, only these broad generalizations can be made, since the results are patient dependent, as shown in Figure 2. To the extent that optimal θ are T1 dependent—and they are field dependent—our results are strictly applicable to 3.5-kG (0.35-T) operation.

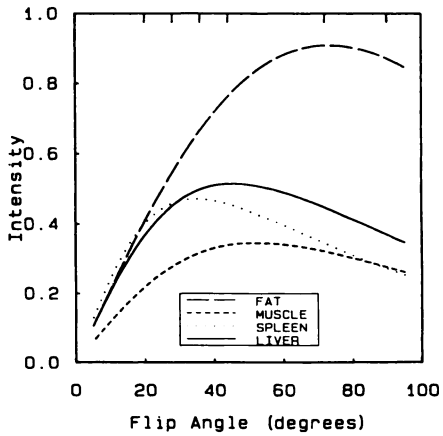

Figure 13. Fitted lines through acquired data (acquisition points indicated by tick marks on top border of the graph) show signal intensities as a function of flip angle in the abdomen of a healthy volunteer; obtained with TR = 0.15 sec, TE = 20 msec.

Finally, we note that good-quality T1 images can be calculated from two short TR procedures with different flip angles, these images requiring a total of 4.2 minutes of acquisition (Fig. 12). The T1 image from partial flip sequences was computed from θ = 90° and 28° images. Similar results were obtained from θ = 90° and 36° images. Compared with the conventionally obtained T1 image, partial flip images require 1/5 the acquisition time and are about 60% noisier. The T1 values from partial flip data are

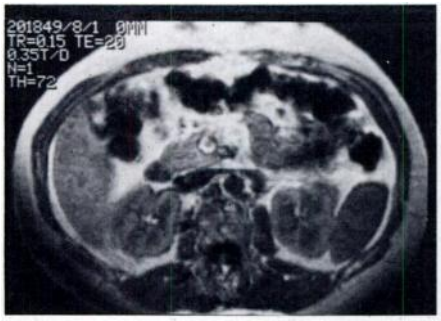

a.

b.

Figure 14. Partial flip image of healthy volunteer described in Figure 13, obtained with 0.15/20, $\theta = 72°$ **(a)** and $\theta = 20°$ **(b)**, $n = 1$, 1.7 × 1.7-mm resolution, 10-mm thickness, and an imaging time of 19 sec (single breathhold). Note loss of tissue contrast in image with smaller flip angle.

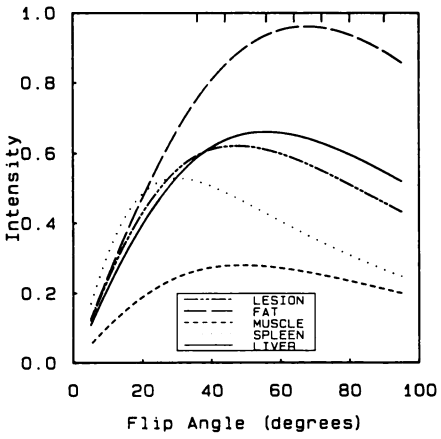

Figure 15. Fitted lines through acquired data (acquisition points indicated by tick marks on top border of the graph) show signal intensities as a function of flip angle for a patient with liver metastasis, obtained with 0.15/20 technique.

about 20% smaller, probably as a result of section profile differences between RF and gradient-reversal refocusing.

Body Imaging

For fast body imaging, partial flip MR imaging can be used to improve S/N. Figure 13 shows acquired signal intensity data as a function of flip angle. We note the characteristic behavior at TR = 0.15 sec, $\theta = 90°$, where

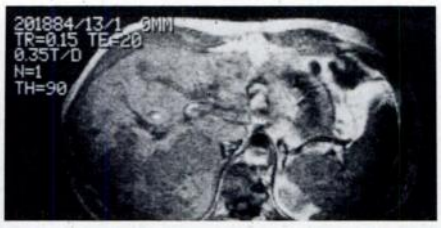

a.

b.

c.

Figure 16. Images of the patient in Figure 15. Flip angles are 90° **(a)**, 72° **(b)**, and 44° **(c)**. Image was obtained with 0.15/20, $n = 1$, 1.7 × 1.7-mm resolution, 10-mm thickness, and an imaging time of 19 sec. Note "flat" appearance and loss of tumor/liver contrast in image obtained with a small flip angle.

fat is most intense, muscle and spleen are of low intensity, and healthy liver is somewhat higher. As flip angle decreases, intensity of imaged fat peaks near 70°. The image intensity of other tissues peaks in the 30°–50° range. Liver and spleen become isointense at 30° and both become isointense with fat at 20°. Figure 14 shows partial flip images in a healthy volunteer. In a patient with liver metastasis, imaging performed with a TR = 0.15 sec technique produced similar intensity behavior for normal tissues (Fig. 15), but below $\theta = 45°$ signal differences started to decrease. Images obtained in this patient are shown in Figure 16.

The behavior of signal intensities demonstrated in Figures 13 and 15 indicates that in the body partial flip images with θ greater than 45° improve S/N for short TR imaging without substantially affecting contrast, but that flip angles should remain above 45° so that image contrast is not degraded. When TE is reduced to 12 msec, phase differences between fat and water produce artifactual lines that clearly outline boundaries between tissues (Fig. 17).

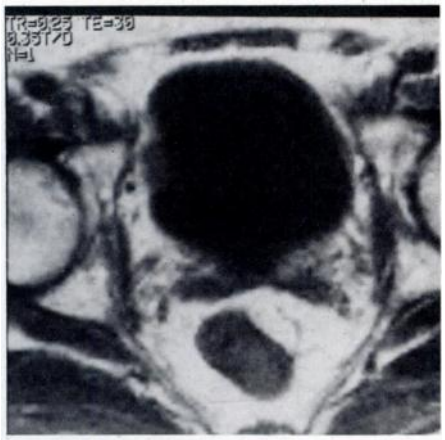

a.

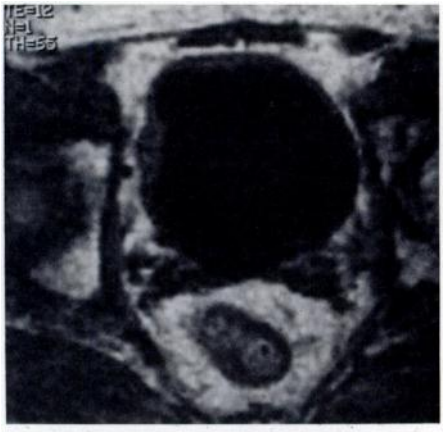

b.

Figure 17. Magnified transverse views of region of the bladder in a patient with a bladder wall tumor. A conventional 0.25/30, $n = 1$, 32-sec image is shown in **a.** Tumor and bladder wall are of intensity intermediate between urine and fat. In a 0.25/12, $n = 1$, and $\theta = 65°$ partial flip image **(b)** a dark line is observed between bladder wall and tumor. This line arises from signal cancellation resulting from fat/water phase differences at TE = 12 msec and 3.5 kG (0.35 T).

These lines are not themselves representative of anatomic features, and care should be taken in interpreting them. Nevertheless, they can provide useful diagnostic information.

DISCUSSION

Partial flip MR imaging provides images with high object contrast for pathologic conditions in which the water content of tissues is increased. Water elevation is accompanied by correlated increases in T1, T2, and N(H) (16, 17). For spin-echo imaging with $\theta = 90°$, lengthening T1 decreases signal intensity, while increasing the other two parameters increases it. As a consequence, lesions do not become brighter than surrounding background until T2 and N(H) effects overshadow T1 effects. This occurs at long TR values. For TR

< T1, as the flip angle is reduced, signal intensity increases, peaks, and decreases. For any one TR, the longer the T1 of the tissue, the smaller the angle at which signal intensity peaks, and the stronger the peak. Therefore, partial flip MR imaging tends to reverse the dependency of signal intensity on T1 effects. (This effect should add further confusion to that already generated by the general use of the misnomer "T1-weighted" for images in which watery lesions appear dark.)

Partial flip imaging with gradient reversals also avoids the very serious problem posed by limits on RF power deposition in high field strength imaging. Currently, considerable efficiency must be sacrificed in multisectional scanning in order for imagers to operate within Food and Drug Administration guidelines; otherwise approval for exceeding FDA limits must be obtained from an Institutional Review Board (18). By depositing only a fraction of the power of normal high field strength imaging methods, partial flip imaging reduces power deposition problems. For instance, a single-echo procedure performed with a flip angle of 45° and gradient reversals for refocusing will deposit 5% of the RF power of a similar procedure performed with θ = 90° and RF refocusing pulses (Appendix B). It should not be surprising, then, if these techniques were to become even more important in high field strength imaging.

Unfortunately, the significant benefits of partial flip MR imaging are accompanied by some disadvantages. If we try to obtain maximum time savings, contrast changes rapidly as a function of θ, which makes careful selection of the partial flip angle critical. Currently, multisectional partial flip MR imaging must be used with gradient reversal refocusing in order to generate the spin echo. It is worth noting that gradient reversals carry distinct disadvantages. This mode of operation is sensitive to background field inhomogeneities, which result not only from magnet and siting factors (which are controllable) but also from the presence of ferromagnetic clips, markers, and prostheses in patients (which are currently uncontrollable). These problems increase with increasing operating magnetic field (19). In principle, however, means for using 180° RF pulses are possible.

Until a more robust implementation of partial flip MR imaging is found, these limitations cannot be overlooked. It is our opinion that, if the patient can tolerate a longer procedure (e.g., 4–5 minutes), a long TR sequence with $n = 1/2$ is preferable. But when imaging time is critical, partial flip MR imaging can cut time by half again, even compared with $n = 1/2$ techniques, and provide about the same SD/N. As for T1 images, since T2 and N(H) data usually are needed also, partial flip MR imaging does not help shorten the total acquisition time. Other applications are possible: For instance, a TR = 1 sec, θ = 26° partial flip technique will produce a "myelogram" effect, with CSF very bright, spine intermediate, and bone dark, an effect that now necessitates imaging with TR = 3,000 msec or longer (12).

It is worth noting as well that the use of analytical tools to model the partial flip technique aids understanding of the process and helps focus experimental work on the most productive combinations of TR, θ parameters. This speeds up research and minimizes time spent on patient imaging.

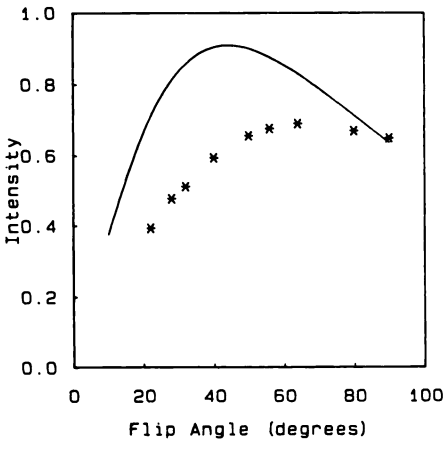

18.

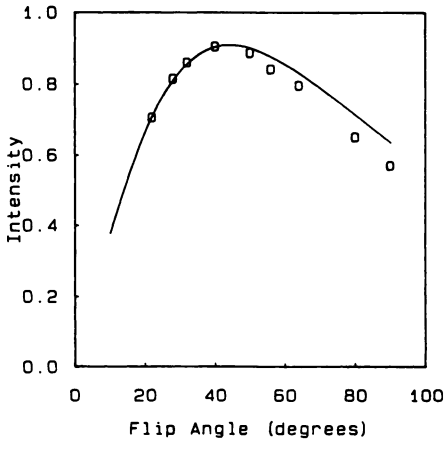

19.

Figures 18, 19. **(18)** Acquired (points) and predicted (line) intensities as a function of flip angle in a phantom, using selective 180° RF pulses. Acquired data fails to show predicted significant increase in signal. **(19)** With use of nonselective 180° RF pulses, acquired (points) and predicted (line) intensities match. This mode of acquisition is restricted to single-section imaging and is therefore impractical.

APPENDIX A

Section Profiles in Partial Flip Imaging

Equation (1) describes the recovery of longitudinal magnetization in the time interval TR. For the case of flip angles equal to 90°it reduces to the familiar form [1 − exp (−TR/T1)]. This relationship assumes that the magnetization regrowth is unperturbed by other RF pulses, which is the case when gradient reversal techniques are used for refocusing. But if RF pulses are used for this purpose (the most often found case in MR imaging), then the signal intensity also becomes dependent on the number and timing of these pulses. For a single echo acquisition the intensity I is

$$I = \frac{N(H) \sin \theta \exp(-TE/T2)}{1 + \cos \theta \exp(-TR/T1)} A, \quad (A1)$$

where $A = 1 + \exp(-TR/T1) - 2 \exp[(TE/2 - TR)/T1]$. For a double-echo procedure,

$$I = \frac{N(H) \sin \theta \exp(-TE/T2)}{1 - \cos \theta \exp(-TR/T1)} B, \quad (A2)$$

where $B = 1 - \exp(-TR/T1) + 2 \exp[(TE/2 - TR)/T1] - 2 \exp[(3TE/2 - TR)/T1]$.

It should be noted that for an odd number of spin echoes the sign of the cosine term in the denominator is positive, which means that the interesting flip angles become those greater than 90°.

Our initial implementation of partial flip angle imaging used RF refocusing and two spin echoes. Initial results for a phantom with a T1 = 1.5 sec are shown in Figure 18. The acquired data are in complete disagreement with predicted values. After eliminating all other sources of error, we found that the use of nonselective 180° RF pulses provided excellent agreement with experimental values (Fig. 19). Computer simulations confirmed that as the flip angle changes from the conventional value of 90° to smaller values, section profiles degrade. For a sequence with a section thickness of 10 mm and selective 180° RF refocusing pulses, signal intensity is quite constant across the section for θ = 90°. This is not the case for a partial flip angle of 45° (Fig. 20). When the same simulation is applied to refocusing by gradient reversals and 45° flips, the section profile recovers its uniformity (Fig. 21), and the experimental results match predictions, as demonstrated above. There are well-understood disadvantages associated with gradient reversals. Although they offer an expedient method to implement partial flip imaging, we be-

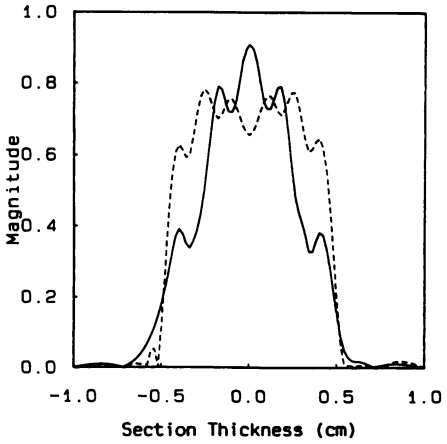

20.

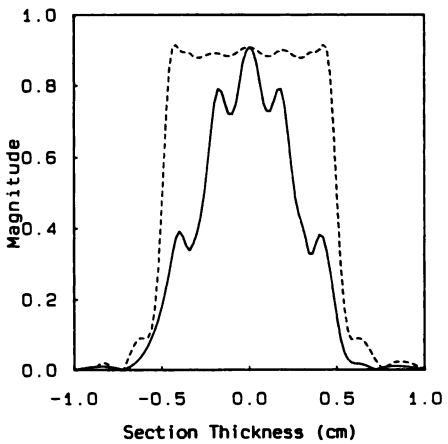

21.

Figures 20, 21. **(20)** Quite uniform profile of a selective 90° flip angle (broken line) becomes degraded for a flip angle of 45° (solid line). These profiles are the result of calculations. **(21)** For a flip angle of 45°, a selective RF refocusing pulse shows poor profile (solid line) in this simulation. Calculations performed with use of the same simulation tools predict that gradient reversals will yield more uniform profiles (broken line).

lieve that it may be possible to shape the 180° RF pulse properly to provide good partial flip results without the disadvantages referred to above.

APPENDIX B

RF Power Deposition

In a conventional spin-echo procedure in which a 90° RF excitation pulse is followed by a 180° refocusing pulse, the latter deposits 4 times more RF power than the former. Thus, if 1 unit of power is used for the 90° pulse, the full sequence utilizes 5 such units. The RF power deposited by the excitation pulse varies as $(\theta/90°)^2$, so that a 45° pulse delivers $1/4$ of a unit. Thus, for a gradient reversal (no 180° RF pulse) procedure with a 45° flip angle the power delivered is $1/4$ unit, versus 5 units for the conventional spin-echo sequence. Thus, in this example, the partial flip procedure uses $1/20$, or 5%, of the power of the conventional sequence. ■

References

1. Lukes SA, Crooks LE, Aminoff MJ, et al. Nuclear magnetic resonance imaging in multiple sclerosis. Ann Neurol 1983; 13:592.
2. Brant-Zawadzki M, Norman D, Newton TH, et al. Magnetic resonance of the brain: the optimal screening technique. Radiology 1984; 152:71-77.
3. Ortendahl DA, Hylton NM, Kaufman L, et al. Analytical tools for magnetic resonance imaging. Radiology 1984; 153:479-488.
4. Droege RT, Wiener SN, Rzeszotarski MS. A strategy for magnetic resonance imaging of the head: results of semi-empirical model. Part II. Radiology 1984; 153:425-433.
5. Crooks LE, Arakawa M, Hoenninger J, et al. Nuclear magnetic resonance whole-body imager operating at 3.5 kGauss. Radiology 1982; 143:169-174.
6. Crooks LE, Ortendahl DA, Kaufman L, et al. Clinical efficiency of nuclear magnetic resonance imaging. Radiology 1983; 146:123-128.
7. Brant-Zawadzki M. Recent advances in MRI of the CNS: contrast agents and spectroscopy. Presented at the Neuroimaging Course, American Academy of Neurology, New Orleans, April 27-May 3, 1986.
8. Modic MT. Magnetic resonance imaging of brain tumors. Presented at the 3rd Annual Magnetic Resonance Imaging 1986: National Symposium, Orlando, Fla., May 5-9, 1986.
9. Feinberg DA, Hale JD, Watts JC, Kaufman L, Mark A. Halving MR imaging time by conjugation: demonstration at 3.5 kG. Radiology 1986; 161:527-531.
10. Haase A, Frahm J, Matthaei D, Hanicke N, Merboldt K. Rapid images and NMR movies. Presented at the 4th Annual Meeting of the Society of Magnetic Resonance in Medicine, London, August 19-23, 1985.
11. Ernst RR, Anderson WA. Application of Fourier transform spectroscopy to magnetic resonance. Rev Sci Instr 1966; 37:93.
12. Mills TC, Ortendahl DA, Hylton NM. Investigation of partial flip angle magnetic resonance imaging. IEEE Trans Nucl Sci 1986; NS-33:496-500.
13. van Uijen CMJ, den Boef JH, Verschuren FJJ. Fast Fourier imaging. Magn Reson Med 1985; 2:203-217.
14. Ortendahl DA, Hylton NM, Kaufman L, Crooks LE. Optimal strategies for obtaining the minimal NMR data set. IEEE Trans Nucl Sci 1985; NS-32:880-884.
15. Dixon T. Simple spectroscopic imaging. Radiology 1984; 153:189-194.
16. Davis PL, Kaufman L, Crooks LE. Tissue characterization. In: Margulis A, Higgins C, Kaufman L, Crooks L, eds. Clinical magnetic resonance imaging. San Francisco: University of California Press, 1983.
17. Crooks LE, Hylton NM, Ortendahl DA, Posin JP, Kaufman L. The value of relaxation times and density measurements in clinical MRI. Invest Radiol (in press).
18. General Electric Company, Medical Systems Group. Signa system operator manual. Milwaukee: General Electric, 1985.
19. Feinberg DA, Crooks LE, Kaufman L. Magnetic resonance imaging performance: a comparison of sodium and hydrogen. Radiology 1985; 156:133-138.